Supplemental Material

Synthesis and antimicrobial activity of knipholone analogs

Melese Legesse[1], Abiy Abebe[2], Sileshi Degu[2], Yonatan Alebachew[1], Solomon Tadesse[1,*]

[1]Department of Pharmaceutical Chemistry and Pharmacognosy, School of Pharmacy, College of Health Sciences, Addis Ababa University, Ethiopia.

[2]Traditional and Modern Medicine Research Directorate, Ethiopian Public Health Institute, Addis Ababa, Ethiopia.

[*]Corresponding author: Tel.: +251911488473; e-mail: solomon.tadesse@aau.edu.et

Abstract

In the present study, we use knipholone as a prototype molecule to identify new anti-infective agents. Since knipholone is insoluble in water, which would have a detrimental effect on its bioavailability and efficacy, we synthesized and determined the *in vitro* antimicrobial activity of knipholone Mannich base derivatives (**2-4**) that have better predicted solubility against eight pathogenic bacterial and fungal strains. The chemical structures of compounds **1-4** were elucidated from their ^{1}H and ^{13}C NMR data, and their antimicrobial activity evaluation was carried out by a broth microdilution MTT assay. Compound **3** exhibited the strongest efficacy against *Staphylococcus epidermidis*, with MIC value of 9.7 µg/mL. While **4** exhibited the best activity against *Staphylococcus aureus*, with an MIC value of 19.5 µg/mL, and was the only one to significantly inhibit the fungus *Trichophyton mentagrophytes* (MIC = 78.2 µg/mL). The study provides evidence for the antibacterial activity of aminoalkyl derivatives of knipholone.

Key words: Antibacterial activity, antifungal activity, *in vitro*, knipholone, Mannich base

Contents

S1 Experimental

1.1 Plant material collection

The rhizomes of *K. foliosa* were collected in February 2021 from mount Kundi near the city of Ankober in Shewa region of Central Ethiopia and identified by Professor Sebsibe Demisew at the National Herbarium, Addis Ababa University (AAU), Addis Ababa, Ethiopia, where voucher specimens were deposited (Collection number: YA01/2017).

1.2 Extraction and isolation of knipholone

The air-dried powdered rhizomes (500 g) of *K. foliosa* were macerated in ethyl acetate at room temperature for 4 days with occasional shaking. The extract was concentrated under vacuum using a rotary evaporator (BUCHI Rotavapor™ R-300, Switzerland) to yield a dark red residue (30 g, 6%). A 4 g portion of the extract was subjected to silica gel column chromatography (400 g, 60 cm length, 40 mm diameter) with gradient elution of EtOAc in toluene; 0:10, 1:9, 1:4, 2:3, 1:1, 3:2, 4:1, resulting in knipholone (**1**, 25 mg).

1.3 Synthesis of knipholone analogs

As shown in scheme 1, three knipholone derivatives (**2-4**) were synthesized by Mannich base reaction using hydrochloric acid as a catalyst. Knipholone, formaldehyde, and amines were refluxed and stirred in isopropanol for 29-30 h to get Mannich base knipholone derivatives (Liu et al. 2014).

1.3.1 1-(3-acetyl-5-((diethylamino)methyl)-2,6-dihydroxy-4-methoxyphenyl)-4,5-dihydroxy-2-methylanthracene-9,10-dione (2)

Compound **2** was synthesized by Mannich base reaction; 23 mg (0.05 mmol) of knipholone (**1**) was dissolved in 50 ml of 2-propanol in a 250 ml round bottom flask, and then 4 ml (50.09 mmol) of 99.5% aqueous diethyl amine, 1.6 ml (18.13 mmol) of 37% aqueous formaldehyde and

small drops of HCl catalyst were added to it. The mixture was stirred for 30 h at 80 ºC. The reaction progress was monitored by analytical TLC using 20% EtOAc in petroleum ether as a solvent system. At the end of the reaction, the solvent was removed, and the reaction mixture was purified by silica gel column chromatography with increasing gradient of EtOAc in petroleum ether as eluting solvent to give **2** as a red amorphous solid (13 mg, 43.44% yield)**.** ^{1}H NMR ((CDCl$_3$)): δ_H 13.71 (1H, *s*, OH, H-1), 12.62 (1H, *s*, OH, H-8), 12.11 (1H, *s*, H-2'), 7.60 (1H, *m*, H-6), 7.58 (1H, *d*, *J* = 3.4 Hz, H-5), 7.28 (1H, *s*, H-2), 7.23 (1H, *m*, H-7), 3.96 (2H, *s*, N-$\underline{CH_2}$), 3.82 (3H, *s*, OCH$_3$), 2.77 (4H, *m*, C-$\underline{CH_2}$), 2.74 (3H, *s*, CO$\underline{CH_3}$), 1.27(3H, *s*, ArCH$_3$), 1.13 (6H, *t*, *J* = 7.1 Hz, C-$\underline{CH_3}$). ^{13}C NMR (125 MHz, (CDCl$_3$): δ_C 202.62 (CO), 192.86 (C-9), 182.43 (C- 10), 164.54 (C-2'), 162.65 (C-4'), 162.09 (C-6'), 161.79 (C-1), 160.56 (C-8), 151.35 (C-3), 136.68 (C-6), 134.89 (C-5a), 131.31 (C-4a), 128.95 (C-4), 125.33 (C-2), 123.36 (C-7), 119.54 (C-5), 115.59 (C-8a), 114.83 (C-1a), 112.08 (C-5'), 107.67 (C-1'), 106.53 (C-3'), 62.58 (4'-O$\underline{C}H_3$), 50.17 (N-$\underline{C}H_2$), 46.05 (C-$\underline{C}H_2$), 30.97 (CO$\underline{C}H_3$), 21.05 (Ar$\underline{C}H_3$), 10.82 (C-$\underline{C}H_3$).

1.3.2 1-(3-acetyl-5-((dimethylamino)methyl)-2,6-dihydroxy-4-methoxyphenyl)-4,5-dihydroxy-2-methylanthracene-9,10-dione (3)

Compounds **3** was prepared following the same procedure as compound **2,** where knipholone (20 mg, 0.05 mmol) dissolved in 40 ml of 2-propanol in a 250 ml Erlenmeyer flask was reacted with 3.2 ml (43.47mmol) of 99.5% aqueous dimethyl amine and 1.3 ml (15.73mmol) of 37% aqueous formaldehyde using 3 drops of concentrated HCl as a catalyst. Then the reaction mixture was stirred for 30 h at 80 ºC. The reaction progress was monitored by TLC using EtOAc in methanol (4:1). Finally, the reaction mixture was purified by silica gel column chromatography with increasing gradient ethyl acetate: methanol (4: 1) as eluting solvents to give compound **3** as a red amorphous solid (14 mg, 61.87% yield). ^{1}H NMR ((CDCl$_3$)): δ_H 13.68 (1H, *s*, OH, H-1),

12.61 (1H, *s*, OH, H-8), 12.10 (1H, *s*, H-2'), 7.74 (1H, *m*, H-6), 7.59 (1H, *d*, *J* = 3.6 Hz, H-5), 7.28 (1H, *s*, H-2), 7.23 (1H, *dd*, *J* = 6.0, 3.5 Hz, H-7), 3.87 (2H, *s*, N-CH_2), 3.82 (3H, *s*, OCH_3), 2.74 (3H, *s*, CO$\underline{CH_3}$), 2.42 (6H, *s*, N-$\underline{CH_3}$), 2.20 (3H, *s*, $ArCH_3$). ^{13}C NMR (125 MHz, ($CDCl_3$): δ_C 202.88 (CO), 193.01 (C-9), 182.57 (C- 10), 163.92 (C-2'), 162.63 (C-6'), 162.10 (C-4'), 161.70 (C-1), 160.46(C-8), 151.27 (C-3), 136.72 (C-6), 134.74 (C-5a), 131.38 (C-4a), 128.85 (C-4), 125.27 (C-2), 123.42 (C-7), 119.64 (C-5), 115.68 (C-8a), 114.95 (C-1a), 112.03 (C-5'), 107.97 (C-1'), 106.59 (C-3'), 62.64(4'-O$\underline{C}H_3$), 55.72 ($\underline{C}H_2$-N), 43.85(N-$\underline{C}H_3$), 31.06(CO$\underline{C}H_3$), 21.06 ($ArCH_3$).

1.3.3 1-(3-acetyl-2,6-dihydroxy-4-methoxy-5-(piperidin-1-ylmethyl)phenyl)-4,5-dihydroxy-2-methylanthracene-9,10-dione (4)

Compound **4** was prepared following the same procedure as above; here 25 mg (0.073 mmol) of knipholone dissolved with 45 ml of 2-propanol in a 250 ml Erlenmeyer flask reacted with 3.7 ml (68.98 mmol) of piperidine and 1.7 ml (24.96 mmol) of 37% aqueous formaldehyde using 3 drops of concentrated HCl as a catalyst. The reaction mixture was stirred for 29h at 80ºC. The reaction progress was monitored by analytical TLC using EtOAc in methanol (4:1), and the reaction mixture was finally purified by silica gel column chromatography with increasing gradient of EtOAc in petroleum ether as eluting solvent to give compound **4** as red amorphous solid. (18mg, 58.84% yield). ^{1}H NMR (($CDCl_3$)): δ_H 13.70 (1H, *s*, OH, H-1), 12.62 (1H, *s*, OH, H-8), 12.11 (1H, *s*, H-2'), 7.59 (1H, *d*, *J* = 4.3 Hz, H-6), 7.58 (1H, *m*, H-5), 7.28 (1H, *s*, H-2), 7.24 (1H, *m*, H-7), 3.86 (2H, *s*, N-$\underline{CH_2}$), 3.81 (3H, *s*, OCH_3), 2.74 (3H, *s*, CO$\underline{CH_3}$), 2.20 (4H, *d*, *J* = 0.9 Hz, CC-$\underline{CH_2}$), 1.63 (2H, *t*, *J* = 26.7 Hz, C-$\underline{CH_2}$-C and $\underline{CH_2}$-CC), 1.27 (3H, *s*, $ArCH_3$). ^{13}C NMR (125MHz, ($CDCl_3$): δ_C 202.81 (CO), 193.03 (C-9), 182.49 (C- 10), 164.18 (C-2'), 162.67 (C-6'), 161.99 (C-4'), 161.80 (C-1), 160.58 (C-8), 151.29 (C-3), 136.70 (C-6), 134.74 (C-5a),

131.60 (C-4a), 128.53(C-4), 125.34 (C-2), 123.40 (C-7), 119.53 (C-5), 115.71 (C-8a), 115.00 (C-1a), 111.95 (C-5'), 107.92 (C-1'), 106.31 (C-3'), 62.53 (4'-O$\underline{C}H_3$), 55.07 (N-$\underline{CH_2}$), 31.06 (CO$\underline{C}H_3$), 29.72 (CC-$\underline{CH_2}$), 25.40 (C-$\underline{C}H_2$-C and $\underline{C}H_2$-CC), 21.01 (ArCH_3).

1.4 Preparation of media, inoculum and standardization

All strains were grown in Petri dishes containing agar medium specific to each microorganism (Arévalo et al. 2003; Nomura et al. 2006). Nutrient media used in the confirmation test of microorganisms and anti-microbial assay was prepared according to the Clinical and Laboratory Standards Institute (CLSI) guideline. The media was sterilized at 121 ^{0}C for 15 minutes using an autoclave and it was cooled to 45-50 ^{0}C in water bath. 20ml of media was poured into 90mm diameter size petri-dishes under aseptic condition inside Bio-safety Cabinet (Bioair instruments, Eurolone Company, Italy) and allowed some time to solidify. Then, 3-5 of bacterial / fungi strain were inoculated with inoculating loop in to Petri dishes containing agar medium. Each bacterial strain was incubated for 18-24 hours at 37 °C and each fungus was incubated for 7 days at 25°C. Standardization was carried out by taking 3-5 inoculums from a fresh, pure culture of the test organism and making a suspension with Muler Hinton Broth (for bacteria) and sabroud dextrose broth (for fungi). The absorbance of the prepared suspension was read by UV-visible spectrophotometer (Thermo Scientific Evolution 60s CAT 840210100) at 625nm with path length of 1cm till the absorbance reading obtained was 0.08 to 0.1 which is proportional to 1×10^8 CFU/ml bacteria and 1×10^6 spores/ml fungi. The standardized suspension was further diluted with appropriate broth to get 1×10^6 CFU/ml and 1×10^5 spore/ml bacteria and fungi, respectively, and these were used to evaluate the antimicrobial activity of the compounds parallel to positive and negative controls.

1.5 Antimicrobial activity study

1.5.1 Broth microdilution MTT assay

The antimicrobial activity of the compounds was assessed by micro-dilution MTT assay method. The test compounds and the standard drugs were prepared in a concentration twice the desired final concentration as they will be diluted with an equal number of bacteria in broth. Briefly, 100 μL of the compounds or the standard drug (columns 1–7) and 100 μL broth (columns 1–8) was introduced into the first wells of row A of a 96-well plate (Figure S5). Thus, row A in columns 1–5 had 200 μL of broth and synthesized compounds, columns 6 and 7 had 200 μL of broth and ciprofloxacin and DMSO (5%), respectively, while column 8 had 100 μL of broth alone. Two-fold serial dilutions using a multichannel micropipette was done systematically down the columns 1–7 (from rows B–L). 100 μL was removed from the starting concentrations (columns 1–7 in row A) and transferred to the next row with the 100 μL broth, properly mixed, and the procedure was repeated up to the last row (L) where the last 100 μL was discarded.

An equal volume (100 μL) of the 1×10^6 CFU/mL bacterial inoculum or 1-5 $\times 10^5$ CFU/mL for fungi was transferred into all the wells to give us the desired final inoculum load of 5×10^5 CFU/mL, 0.5-2.5 $\times 10^4$ CFU/mL for bacteria and fungi, respectively. Column 8 served as growth control (drug-free). The concentrations of the compounds ranged from 2.5 mg/mL to 1.22 µg/mL, whereas those of the standard drugs ciprofloxacin and amphotericin B ranged from 25 µg/ml to 0.122 µg/ml. Microtiter plates were incubated at 37 °C for 18–24 hrs. Then 40 μL of MTT was added into all 96 well plates and incubated at 37 °C for bacteria and 25 °C for fungi for 30 minutes. The MIC values were determined as the lowest concentration of active compound at which disappearing purple colour was observed (Ohikhena et al., 2017). All the experiments were carried out in triplicate.

MIC is least concentration of the compounds that inhibit growth of microorganisms. It was determined visually as the lowest concentrations of the compounds at which disappearing purple color was recorded as MIC value of bacterial/fungal strains in the MTT broth assay.

1.6 *In silico* prediction

The physicochemical, pharmacokinetic and toxicity profiles of the compounds was estimated using absorption, distribution, metabolism, excretion and toxicity (ADMETlab 2.0) online software tools (Xiong et al. 2021). The molecular docking study of the compounds was carried out using Glide docking module of the Schrödinger suite 2021 version 2 (Schrödinger Inc., New York, USA). The crystal structure of *Staphylococcus aureus* gyrase B (GyrB) bound with a natural product antibiotic novobiocin (PDB: 4URN) was retrieved from the Protein Data Bank and used as a template for the docking (Lu et al. 2014). There were no missing residues in the area around the binding site of protein 4URN. By assigning bond orders, adding any missing hydrogen atoms, disulphide bonds, and removing water molecules longer than 5 Å, the protein was prepared using the protein preparation wizard. To prepare and select the binding site for the docking, Glide was applied to generate a grid by selecting atoms of the bound ligand, novobiocin, in a 20 Å box. The ligand compounds were prepared using the ligprep wizard in Schrödinger suites, and they were subsequently docked following Glide extra precision (XP). The top dock score poses of the compounds were further analyzed and visually inspected using PyMOL to examine their detailed binding interaction (Khair et al. 2019; Davis et al. 2022).

1.7 Statistical analysis

Data analysis was carried out using IBM SPSS (Statistical Package for Social Sciences) Statistics for Windows, Version 20.0. Armonk, NY: IBM Corp. Results was expressed as mean of three replicates. Statistical significance was determined by one-way ANOVA followed by Tukey post

hoc test to compare MIC values of the compounds antimicrobial activity among the treatment and control groups. $P < 0.05$ was considered significant.

Figure S1: The ^{1}H, ^{13}C NMR and DEPT-135 spectra of compound 1 (knipholone).

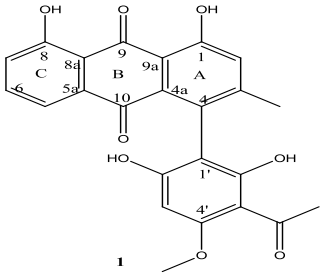

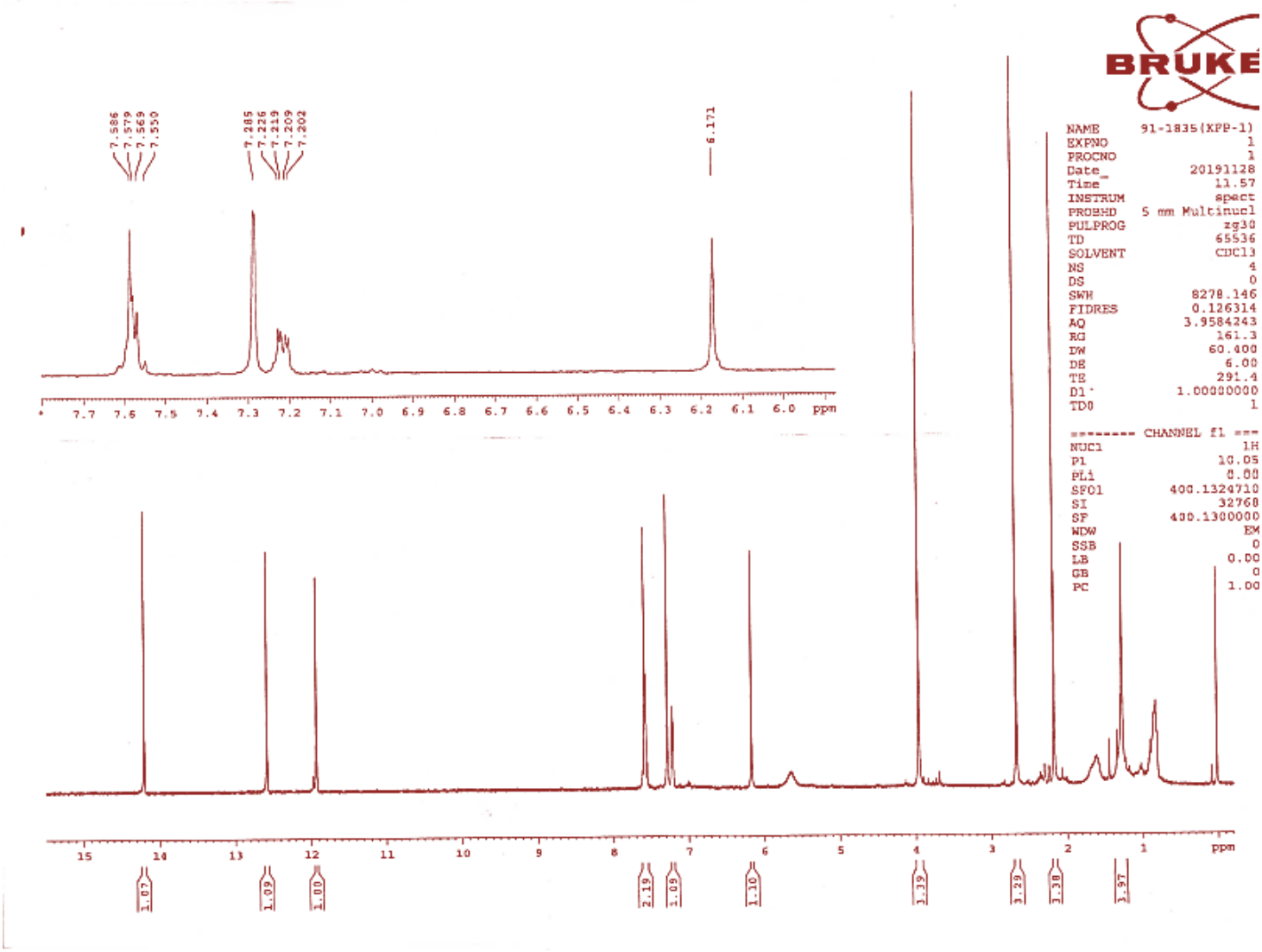

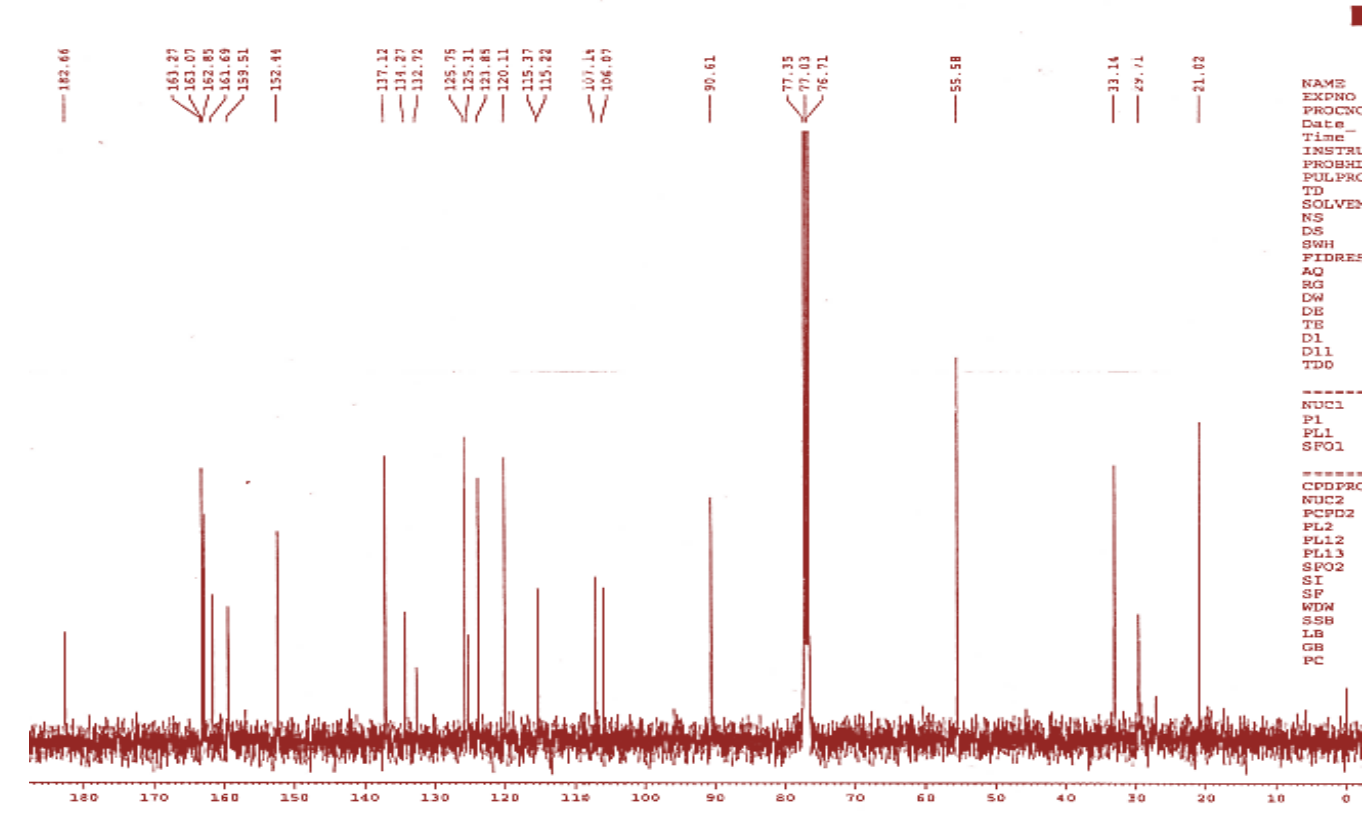
182.66
163.27
163.07
162.85
161.69
159.51
152.44
137.12
134.27
132.72
125.75
125.31
123.85
120.11
115.37
115.22
107.14
106.07
90.61
77.35
77.03
76.71
55.58
33.14
29.71
21.02
NAME
EXPNO
PROCNO
Date_
Time
INSTRU
PROBHD
PULPRO
TD
SOLVEN
NS
DS
SWH
FIDRES
AQ
RG
DW
DE
TE
D1
D11
TD0
NUC1
P1
PL1
SFO1
CPDPRG
NUC2
PCPD2
PL2
PL12
PL13
SFO2
SI
SF
WDW
SSB
LB
GB
PC
180
170
160
150
140
130
120
110
100
90
80
70
60
50
40
30
20
10
0

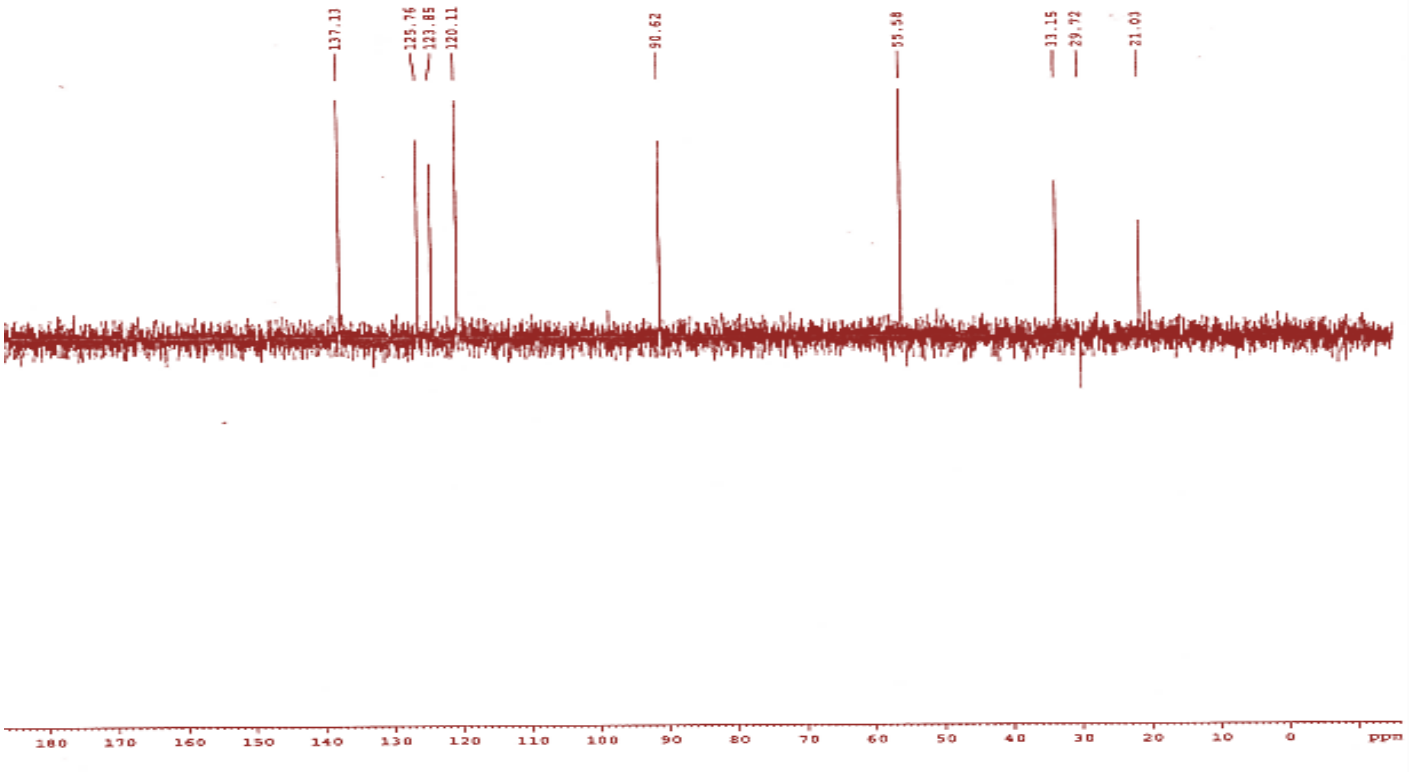
137.13
125.76
123.85
120.11
90.62
55.58
33.15
29.72
21.03
180
170
160
150
140
130
120
110
100
90
80
70
60
50
40
30
20
10
0
ppm

Figure S2: The ^{1}H, ^{13}C NMR and DEPT-135 spectra of compound 2.

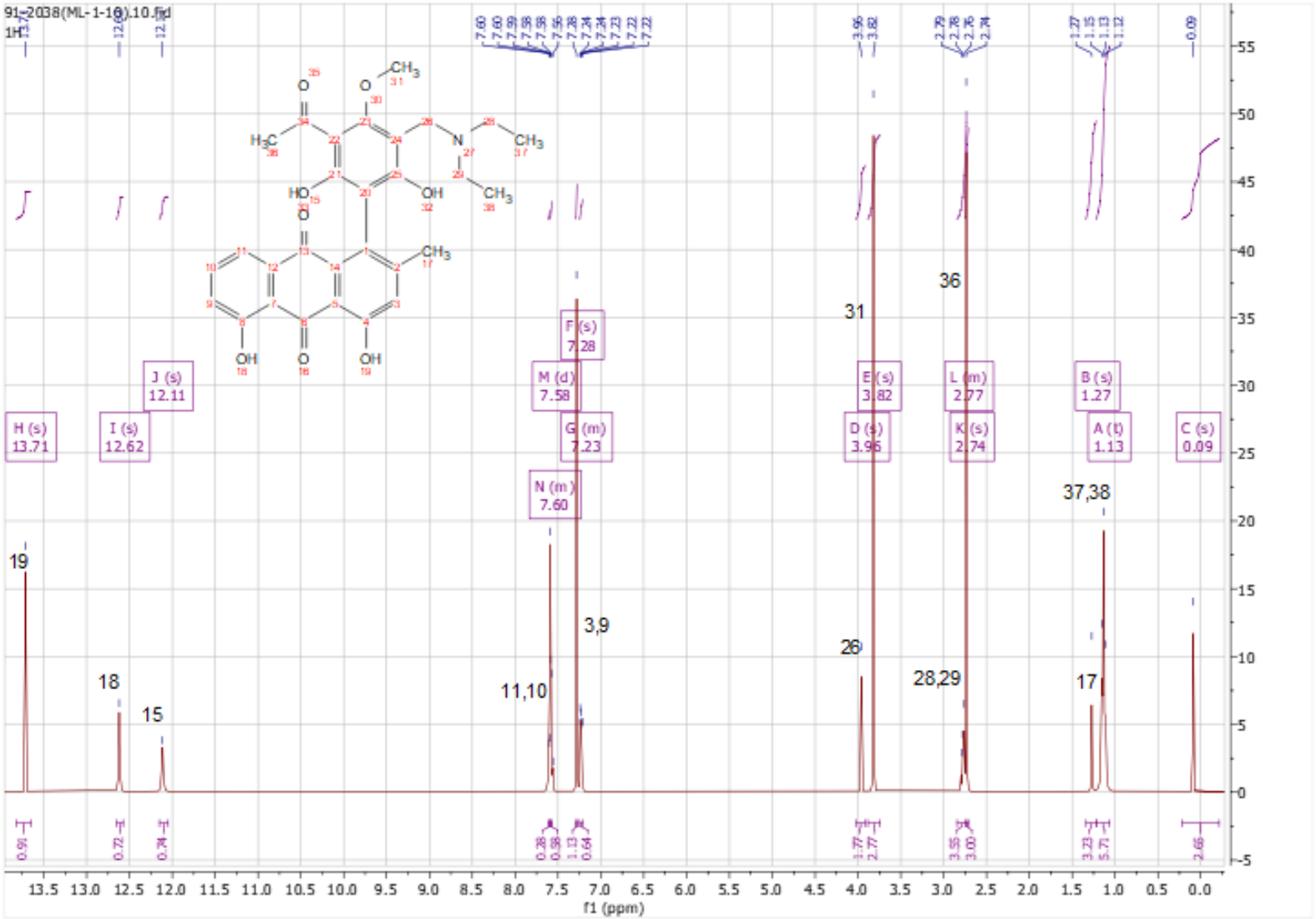

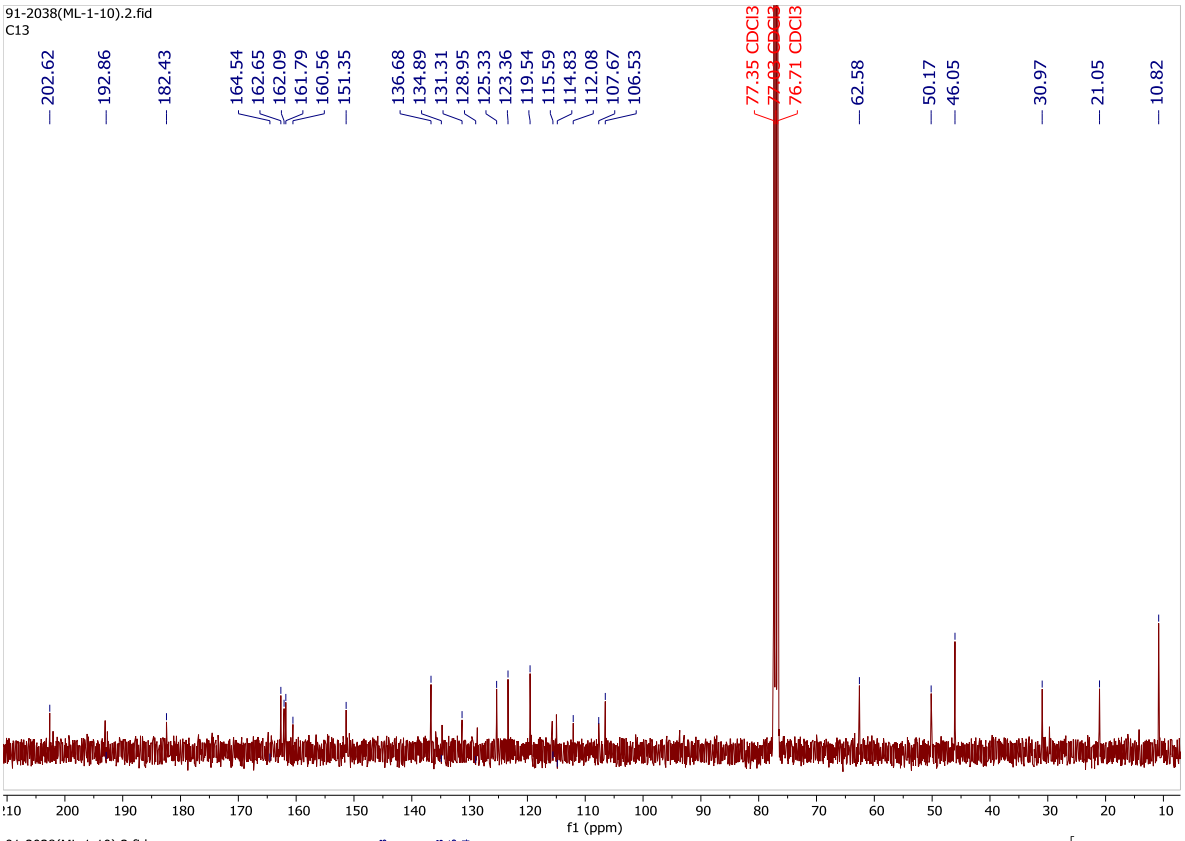
91-2038(ML-1-10).2.fid
C13
202.62
192.86
182.43
164.54
162.65
162.09
161.79
160.56
151.35
136.68
134.89
131.31
128.95
125.33
123.36
119.54
115.59
114.83
112.08
107.67
106.53
77.35 CDCl3
77.03 CDCl3
76.71 CDCl3
62.58
50.17
46.05
30.97
21.05
10.82
f1 (ppm)

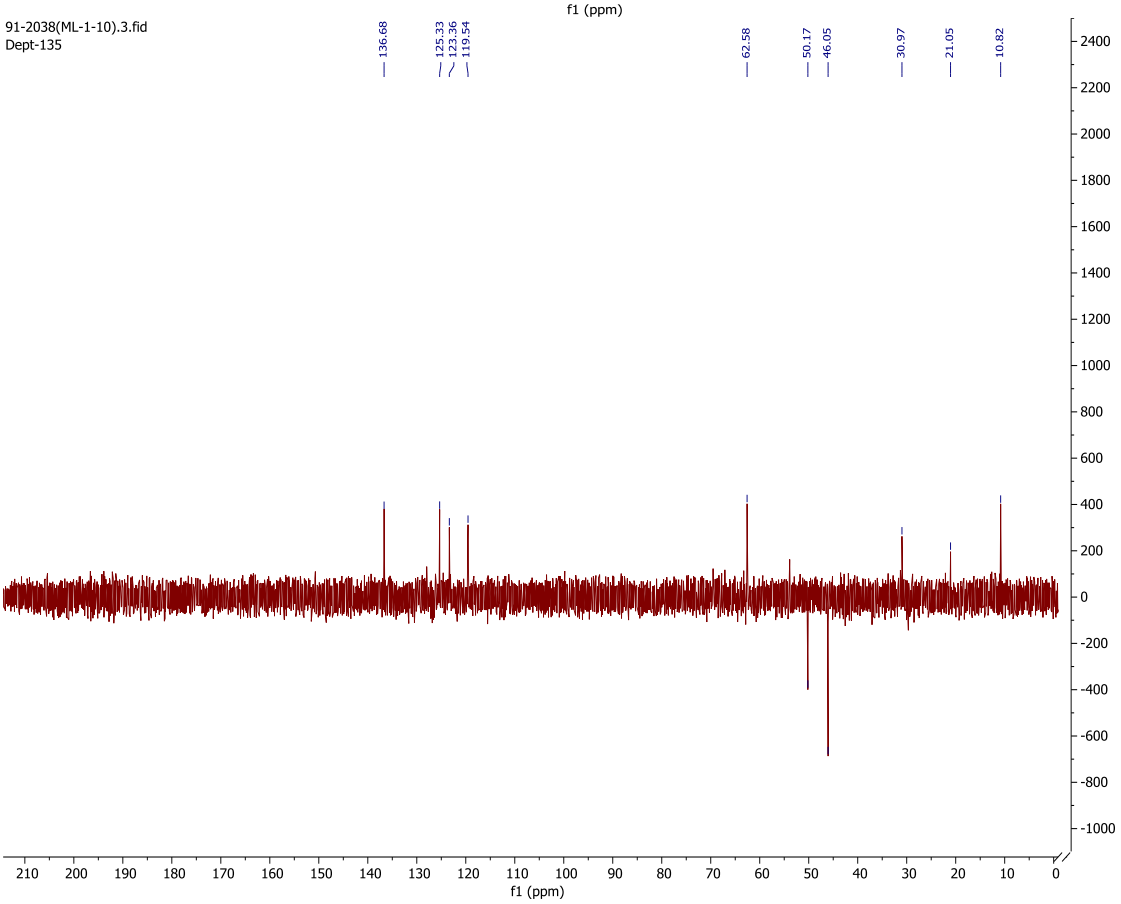
91-2038(ML-1-10).3.fid
Dept-135
136.68
125.33
123.36
119.54
62.58
50.17
46.05
30.97
21.05
10.82
f1 (ppm)

Figure S3: The ^{1}H, ^{13}C NMR and DEPT-135 spectra of compound 3.

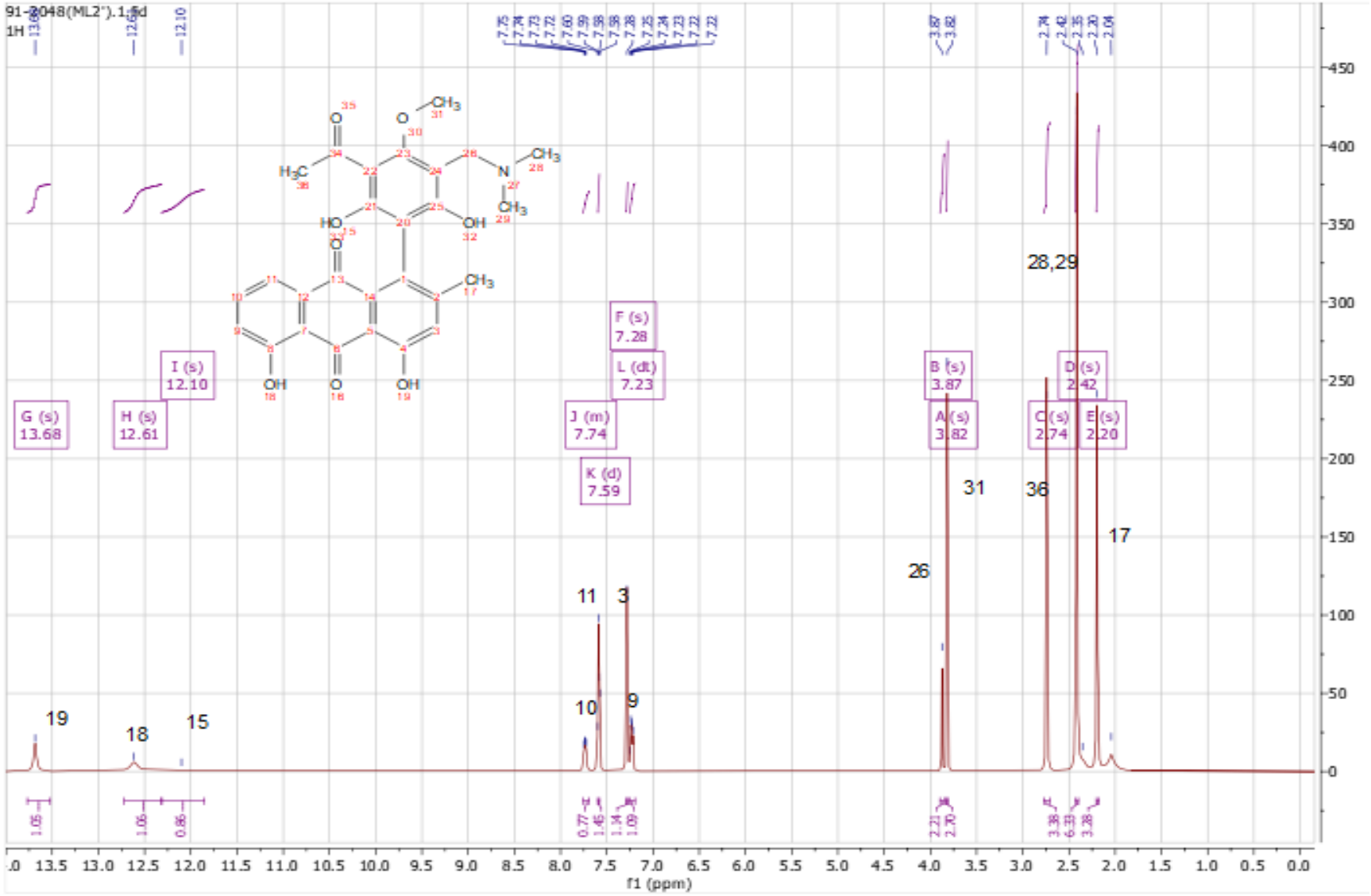

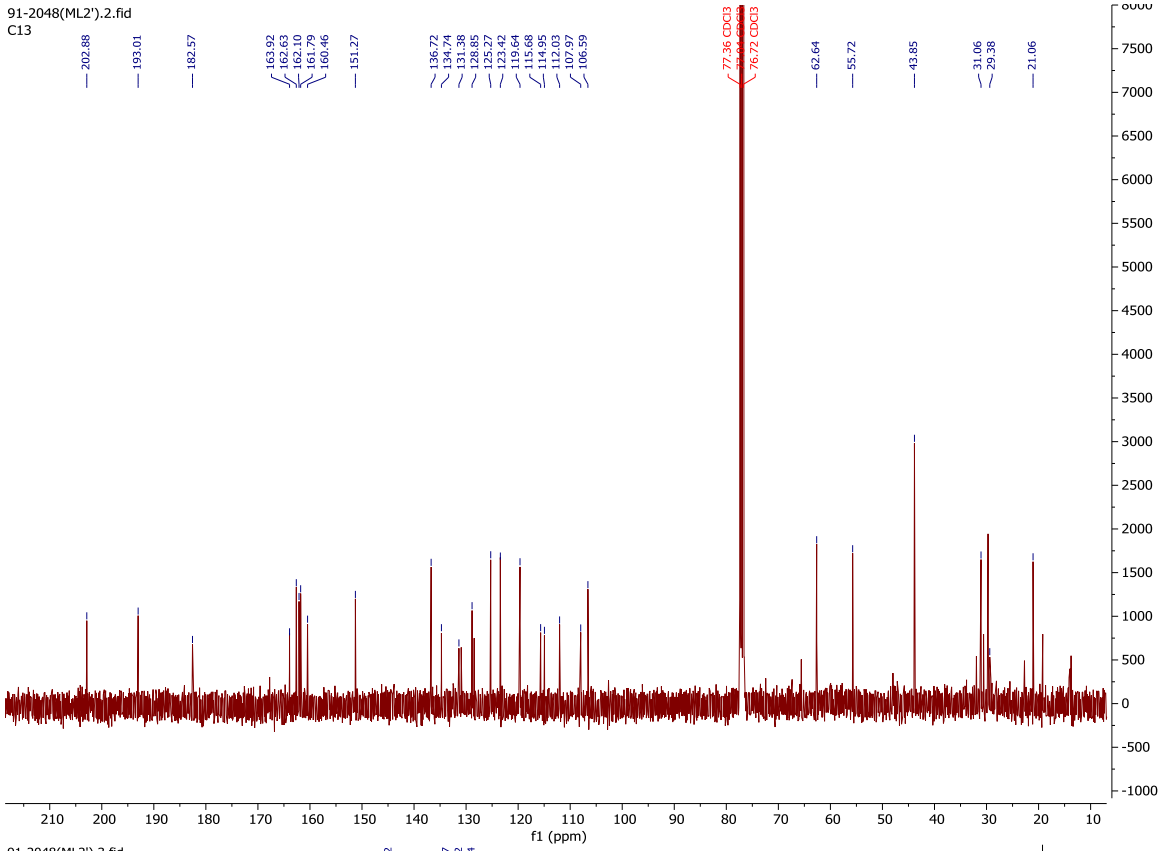
91-2048(ML2').2.fid
C13
202.88
193.01
182.57
163.92
162.63
162.10
161.79
160.46
151.27
136.72
134.74
131.38
128.85
125.27
123.42
119.64
115.68
114.95
112.03
107.37
106.59
77.36 CDCl3
76.72 CDCl3
62.64
55.72
43.85
31.06
29.38
21.06
f1 (ppm)

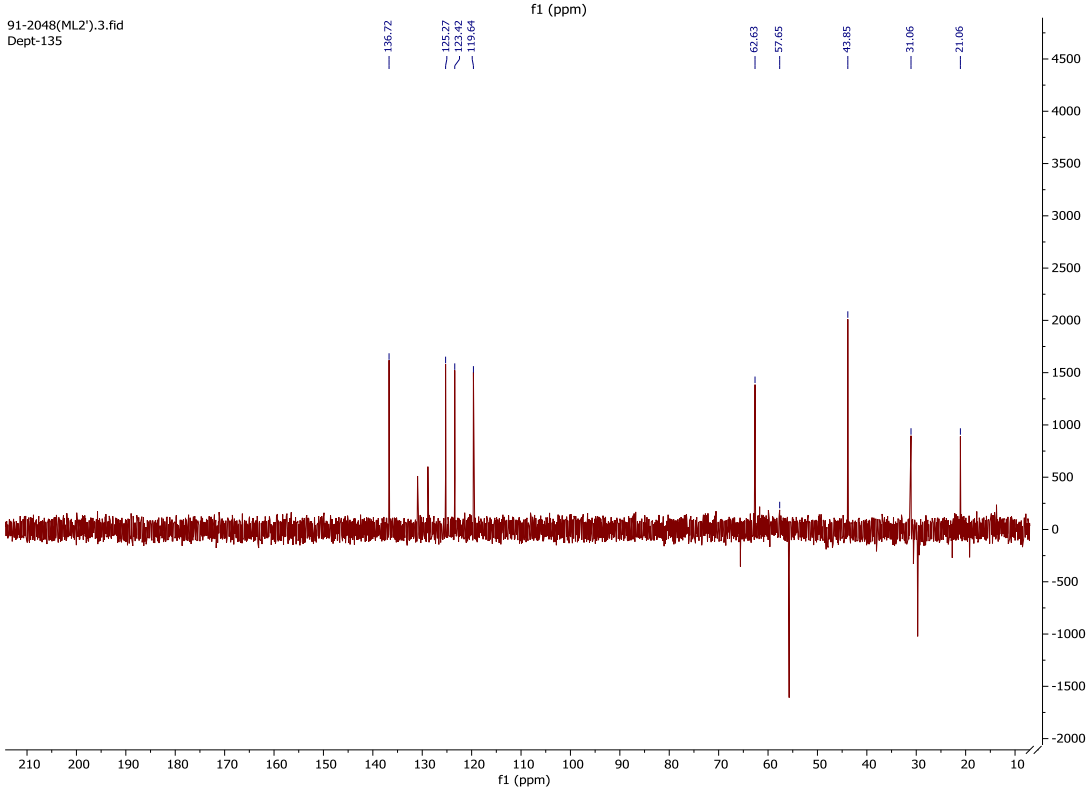
91-2048(ML2').3.fid
Dept-135
136.72
125.27
123.42
119.64
62.63
57.65
43.85
31.06
21.06
f1 (ppm)

Figure S4: The ^{1}H, ^{13}C NMR and DEPT-135 spectra of compound 4.

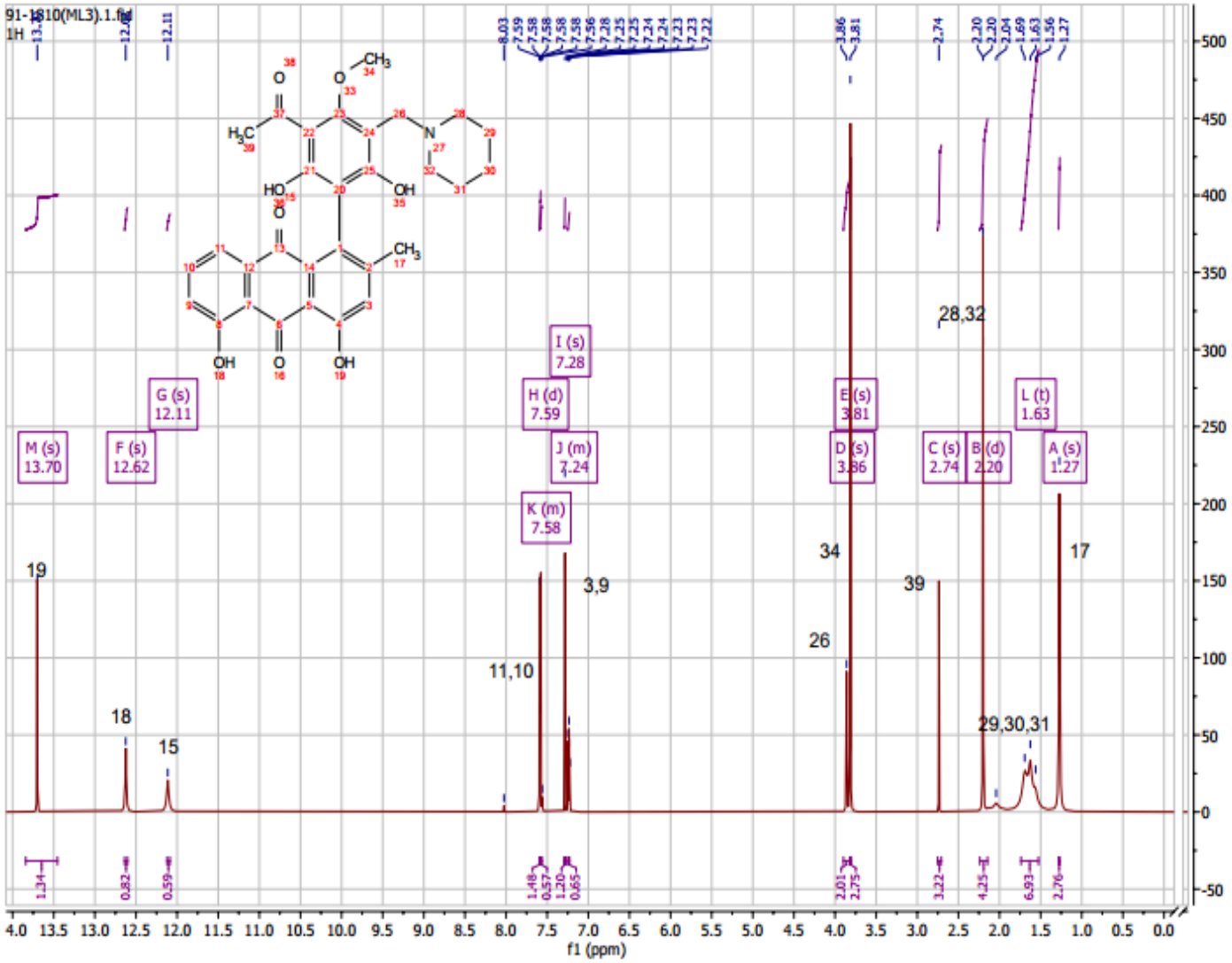

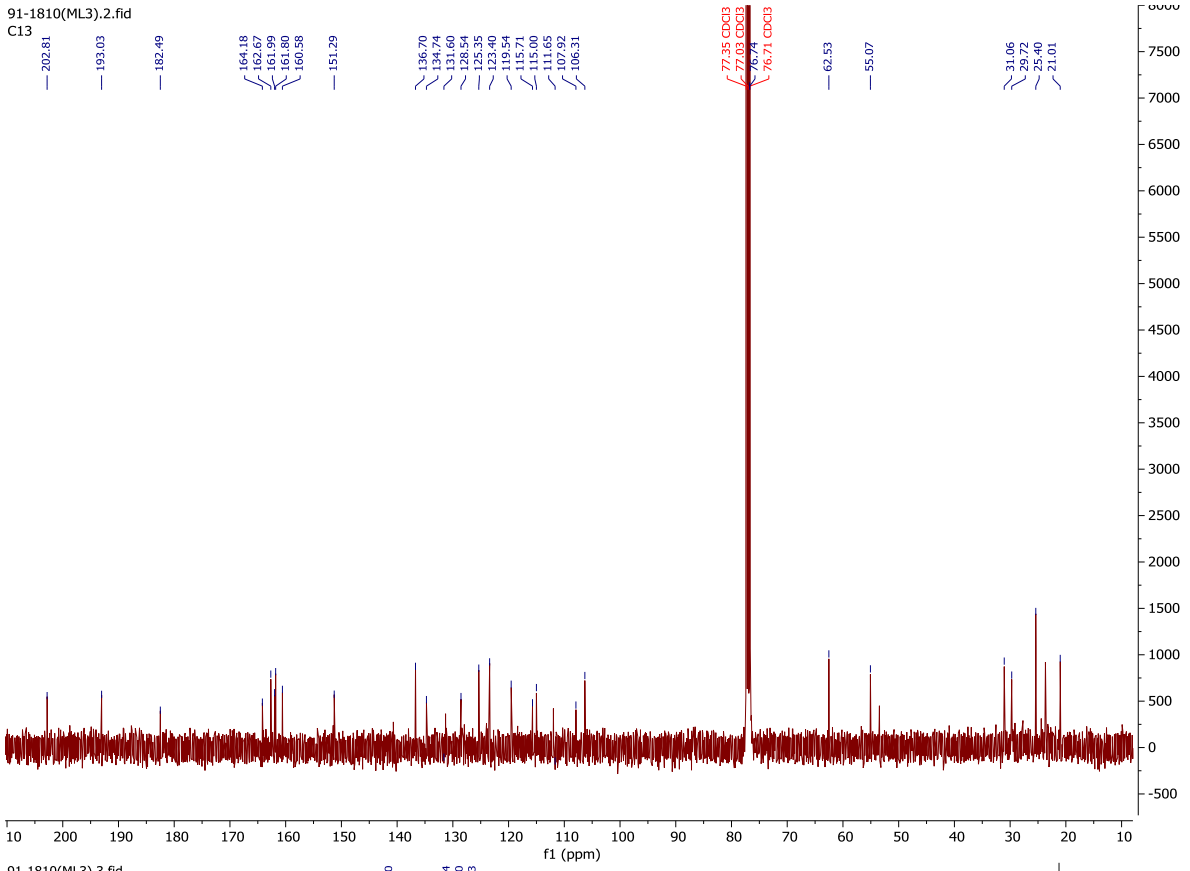
91-1810(ML3).2.fid
C13
202.81
193.03
182.49
164.18
162.67
161.99
161.80
160.58
151.29
136.70
134.74
131.60
128.54
125.35
123.40
119.54
115.71
115.00
111.65
107.92
106.31
77.35 CDCl3
77.03 CDCl3
76.74
76.71 CDCl3
62.53
55.07
31.06
29.72
25.40
21.01
f1 (ppm)

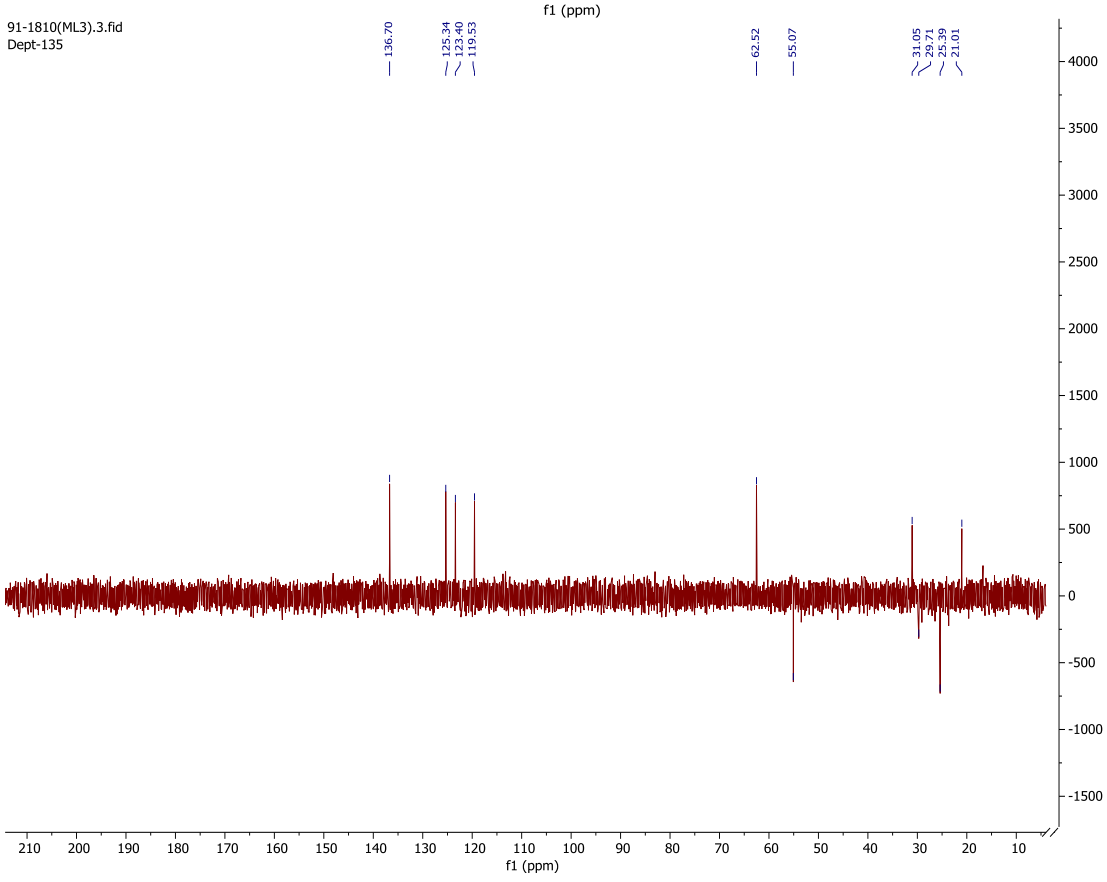
91-1810(ML3).3.fid
Dept-135
136.70
125.34
123.40
119.53
62.52
55.07
31.05
29.71
25.39
21.01
f1 (ppm)

Figure S5: Determination of the MIC value of the compounds in 96 micro-well plate in different microorganism

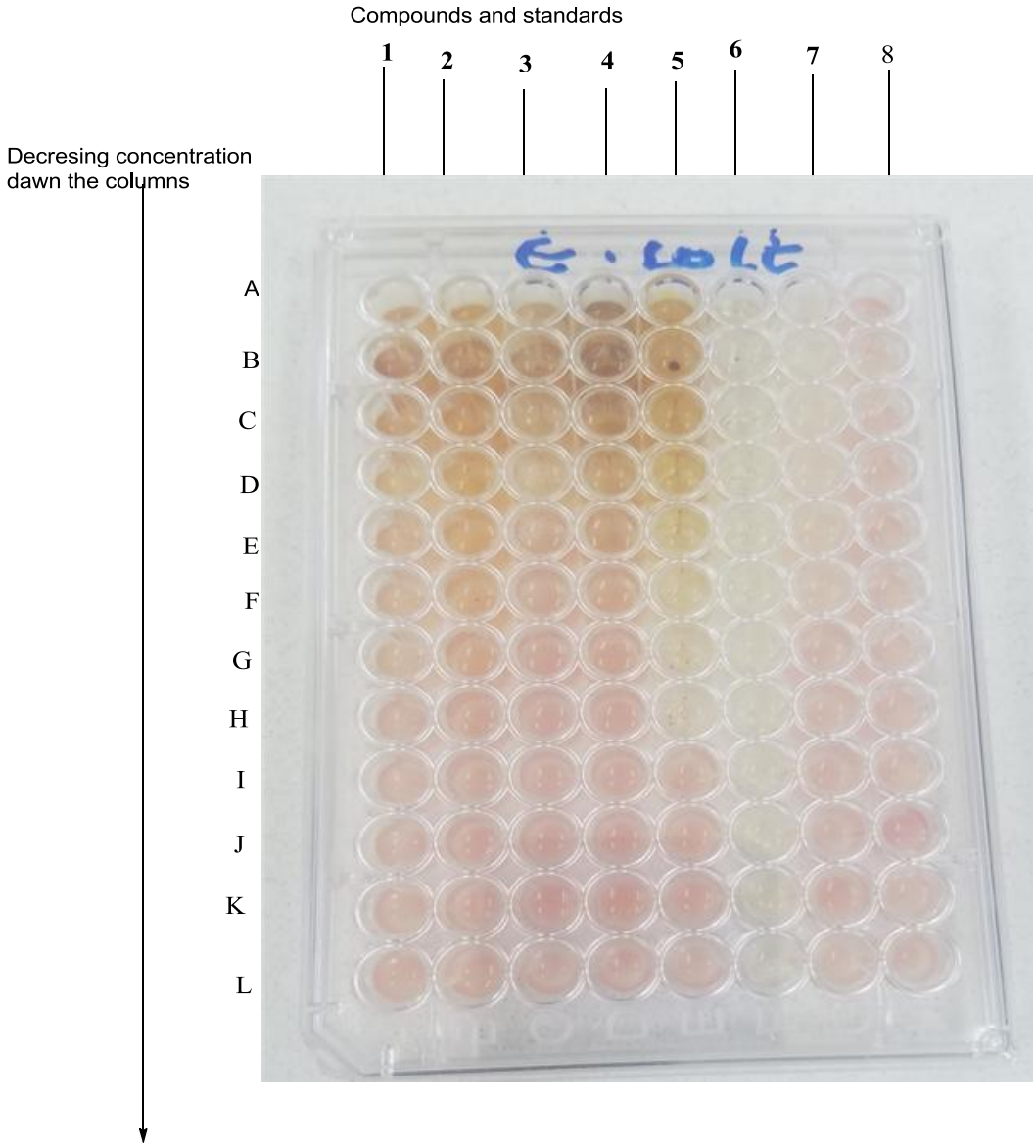

Note: A schematic representation of the 96-well MTT broth microdilution model. Annotations: The yellowish coloration indicates inhibition of growth; purple indicates that organisms are active. 1=knipholone,2=compound 2,3=compound 3,4=compound 4,5=impure 6=positive control (ciprofloxacillin),7=negative control (DMSO) and 8=growth control

Figure S6: MIC value of compounds (**1-4**) and the standard drug ciprofloxacillin against selected bacterial strains. Data are presented as mean of three replicates; n =3.

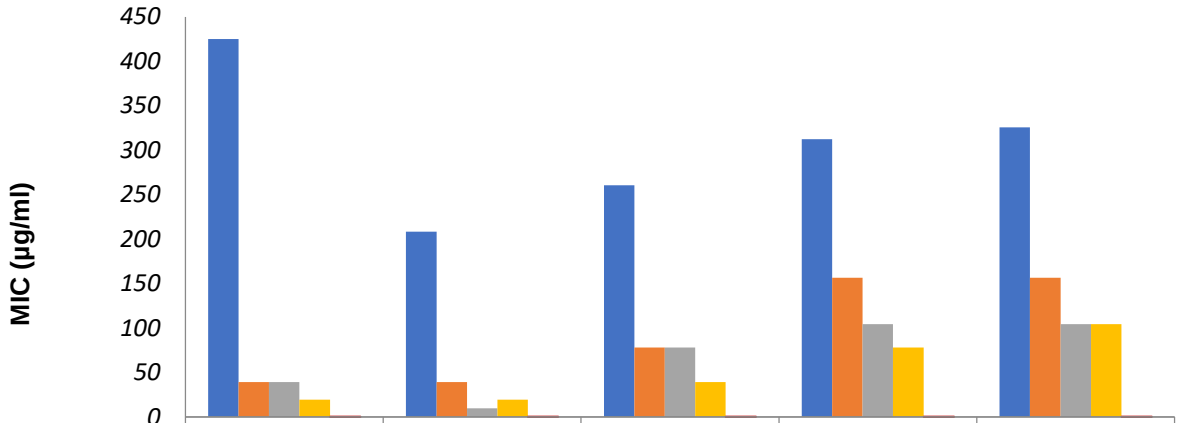

	S. aureus	*S. epidermidis*	*P. mirabilus*	*E. coli*	*P. aeruginosa*
1	425	208.3	260.4	312.5	325.5
2	39.1	39.1	78.1	156.3	156.3
3	39.1	9.7	78.1	104.2	104.2
4	19.5	19.5	39.1	78.1	104.2
Ciprofloxacin	0.097	0.012	0.012	0.012	0.012

Figure S7: The binding modes of compound **4** with *Staphylococcus aureus* DNA gyrase (PDB 4URN). A) The 2D plot and B) Ribbon diagram showing binding interaction of compound **4** with amino acid residues of DNA gyrase. Hydrogen bond is shown in black dotted line and salt bridge is shown in blue solid line.

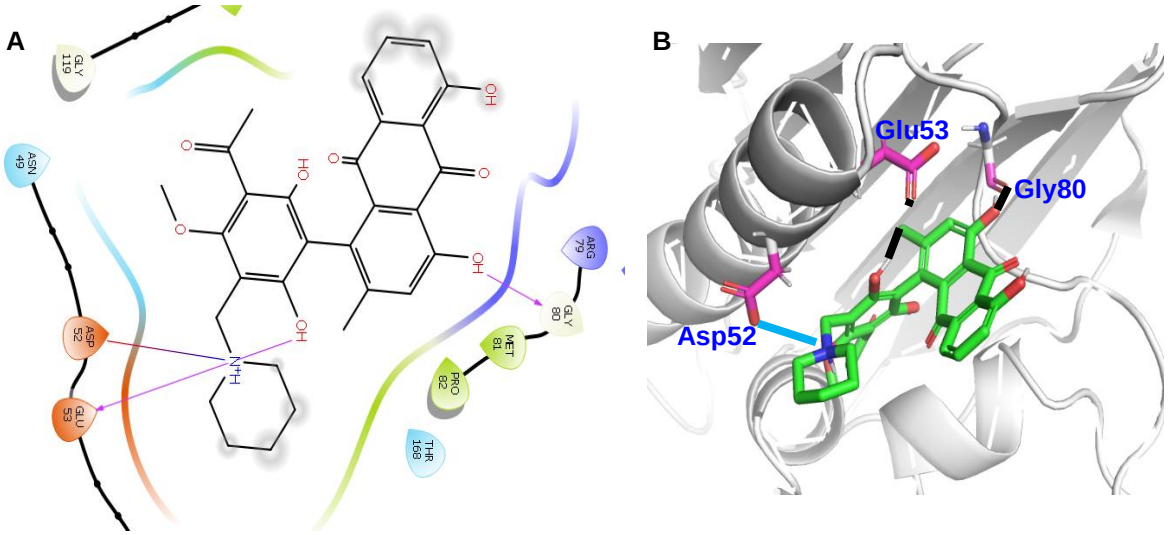

Table S1: ^{1}H and ^{13}C NMR data of knipholone 1 and compounds 2 in chloroform-d

Knipholone (**1**)			Compound **2**	
Position	δ_C (ppm)	δ_H (ppm)	δ_C (ppm)	δ_H (ppm)
1	161.69	12.6 (1H, *s*, -OH)	161.79	13.71 (1H, *s*, -OH)
1a	115.22	-	114.83	-
2	125.31	7.28 (1H, *s*)	125.33	7.28(1H, *s*)
3	152.44	-	151.35	
4	125.75	-	128.95	
4a	132.72	-	131.31	
5	120.11	7.55 (1H, *dd*, *J* = 7, 1.5 Hz)	119.54	7.58(1H, *d*, *J* = 3.4 Hz)
5a	134.27	-	134.89	
6	137.12	7.57 (1H, *dd*, *J* = 8, 7 Hz)	136.68	7.60 (1H, *m*)
7	123.85	7.21 (1H, *dd*, *J* = 8, 1.5 Hz)	123.36	7.23 (1H, *m*)
8	159.51	11.9 (1H, *s*, -OH)	160.56	12.62 (1H, *s*, -OH)
8a	115.37	-	115.59	-
9	192.68	-	192.86	-
10	182.66	-	182.43	-
1’	106.07	-	107.67	-
2’	163.27	5.7 (1H, *s* (*br*), -OH)	164.54	12.11 (1H, *s*, -OH)
3’	107.14	-	106.53	-
4’	163.07	-	162.65	-
5’	90.61	6.19 (1H, *s*)	112.08	-
6’	162.85	14.3 (1H, *s*, -OH)	162.09	-
$ArCH_3$	21.02	2.21 (3H, *s*)	21.05	1.27 (3H, *s*)
OCH_3	55.56	3.91 (3H, *s*)	62.58	3.82 (3H, *s*)
$CO\underline{CH_3}$	33.14	2.70 (3H, *s*)	30.97	2.74 (3H, *s*)
$\underline{C}OCH_3$	202.3	-	202.62	-
N-$\underline{CH_2}$	-	-	50.17	3.96 (2H, s)
C-$\underline{CH_2}$	-	-	46.05	2.77 (2H, *m*)
C-$\underline{CH_2}$	-	-	46.05	2.77 (2H, *m*)
C-$\underline{CH_3}$	-	-	10.82	1.13 (3H, *t*, *J* = 7.2 Hz)
C-$\underline{CH_3}$	-	-	10.82	1.13 (3H, t, J = 7.2 Hz)

s = singlet, *d* = doublet, *dd* = doublet of doublets, *m* = multiplate, *br* = broad.

Table S2: ^{1}H and ^{13}C NMR data of compounds 3 and 4 in chloroform-d

Compound **3**			Compound **4**	
Position	δ_C (ppm)	δ_H (ppm)	δ_C (ppm)	δ_H (ppm)
1	161.79	13.68 (1H, *s*, -OH)	161.80	13.70 (1H, *s*, -OH)
1a	114.95	-	115.00	-
2	125.27	7.28 (1H, *s*)	125.35	7.28 (1H, *s*)
3	151.27	-	151.29	
4	128.85	-	128.54	
4a	131.38	-	131.60	
5	119.64	7.59 (1H, *d*, *J* = 3.6 Hz)	119.54	7.58 (1H, *m*)
5a	134.74		134.74	
6	136.72	7.74 (1H, *m*)	136.70	7.59 (1H, *d*, *J* = 4.3 Hz)
7	123.42	7.23 (1H, *dd*, *J* = 6.0, 3.5 Hz)	123.40	7.24 (1H, *m*)
8	160.46	12.61 (1H, *s*, -OH)	160.58	12.62 (1H, *s*, -OH)
8a	115.68	-	115.71	-
9	193.01	-	193.03	-
10	182.57	-	182.49	-
1’	107.97	-	107.92	-
2’	163.92	12.10 (1H, *s*, -OH)	164.18	12.11 (1H, *s*, -OH)
3’	106.59	-	106.31	-
4’	162.10	-	161.99	-
5’	112.03	-	111.65	-
6’	162.63	-	162.67	-
$ArCH_3$	21.06	2.20 (3H, *s*)	21.01	1.27 (3H, *s*)
OCH_3	62.64	3.82 (3H, *s*)	62.53	3.81 (3H, *s*)
$CO\underline{CH_3}$	31.06	2.74 (3H, *s*)	31.06	2.74 (3H, *s*)
$\underline{C}OCH_3$	202.88	-	202.81	-
N-$\underline{CH_2}$	55.72	3.87 (2H, *s*)	55.07	3.86 (2H, *s*)
N-$\underline{CH_3}$	43.85	2.42 (3H, *s*)	-	-
N-$\underline{CH_3}$	43.85	2.42 (3H, *s*)	-	-
CC-$\underline{CH_2}$			29.72	2.20 (2H, *d*, *J* = 0.9 Hz)
CC-$\underline{CH_2}$			29.72	2.20 (2H, *d*, *J* = 0.9 Hz)
C-$\underline{CH_2}$-C			25.40	1.63 (2H, *t*, *J* = 26.7 Hz)
C-$\underline{CH_2}$-C			25.40	1.63 (2H, *t*, *J* = 26.7 Hz)
$\underline{CH_2}$-CC			25.40	1.63 (2H, *t*, *J* = 26.7 Hz)

s = singlet, *d* = doublet, *dd* = doublet of doublets, *m* = multiplet, *br* = broad.

Table S3: Antifungal activity of compounds **1**-**4**.

Compounds	Minimum Inhibitory Concentration (µg/mL)		
	T. menta	*A. niger*	*C. albicanus*
1	325.5	NA	NA
2	325.5	1666.7	NA
3	325.5	625.0	NA
4	78.2	625.0	NA
Amphotericin B	0.195	0.391	0.097
DMSO (5%)	NA	NA	NA

Data are presented as mean of three replicates; n =3; NA = not active.

Table S4: Physicochemical, pharmacokinetic and toxicity profile prediction of knipholone 1 and its derivatives (2-4) carried out using ADMETlab 2.0 software.

Compounds	Log P	Log S	Log D	F (20%)	Caco-2	BBB	VDss	CL	T1/2	CYP3A4 substrate	CYP3A4 inhibition	CYP2D6 inhibition	CYP2D6 substrate	hERG	Ames	DILI
1	3.47	-7.158	3.253	0.048	-5.867	0.004	0.307	4.458	0.032	0.119	0.26	0.021	0.178	0.021	0.73	0.982
2	2.90	-4.756	1.529	0.065	-5.976	0.006	0.463	8.223	0.016	0.21	0.121	0.012	0.205	0.562	0.711	0.977
3	2.12	-5.444	1.187	0.009	-5.976	0.008	0.999	7.887	0.016	0.25	0.109	0.006	0.231	0.218	0.667	0.980
4	3.58	-4.641	2.742	0.879	-6.028	0.005	0.628	5.088	0.008	0.16	0.094	0.017	0.201	0.529	0.719	0.979

Log P = partition coefficient, Log S = aqueous solubility, insoluble <−10 < poorly <−6 <moderately <−4 <soluble <−2 <very <0 <highly; Log D=n-octanol/water distribution coefficients at pH=7.4, 1- 3 considered proper; F20% = human oral bioavailability 20%, 0-0.3: excellent, 0.3-0.7: medium, 0.7-1.0(++): poor; Caco-2 = human colon adenocarcinoma cell lines, >-5.15, proper; Pgp-sub = P-glycoprotein substrate, 0-0.3: excellent, 0.3-0.7: medium, 0.7-1.0(++): poor; BBB = blood–brain barrier, 0-0.3: excellent; 0.3-0.7: medium; 0.7-1.0(++): poor; VD = Volume distribution, CYP = cytochrome P450, category 0: Non-substrate / Non-inhibitor, category 1: substrate / inhibitor, the probability of being substrate / inhibitor, within the range of 0 to 1; CL = clearance of a drug, 0-0.3: excellent, 0.3-0.7: medium, 0.7-1.0(++): poor; hERG = human ether-a-go-go related gene, 0-0.3: excellent, 0.3-0.7: medium, 0.7-1.0(++): poor; AMES = a test for mutagenicity, 0-0.3: excellent, 0.3-0.7: medium, 0.7-1.0(++): poor; DILI = drug-induced liver injury, 0-0.3: excellent, 0.3-0.7: medium, 0.7-1.0(++): poor.

References

Arévalo MP, Carrillo-Muñoz AJ, Salgado J, Cardenes D, Brió S, Quindós G, Espinel-Ingroff A. 2003. Antifungal activity of the echinocandin anidulafungin (VER002, LY-303366) against yeast pathogens: a comparative study with M27-A microdilution method. J Antimicrob Chemother. 51(1):163-6.

Davis OA, Cheung KJ, Brennan A, Lloyd MG, Rodrigues MJ, Pierrat OA, Collie GW, Le Bihan YV, Huckvale R, Harnden AC, et al. 2022. Optimizing shape complementarity enables the discovery of potent tricyclic BCL6 inhibitors. J Med Chem. 65(12):8169-8190.

Khair NZ, Lenjisa JL, Tadesse S, Kumarasiri M, Basnet SKC, Mekonnen LB, Li M, Diab S, Sykes MJ, Albrecht H, et al. 2019. Discovery of CDK5 inhibitors through structure-guided approach. ACS Med Chem Lett. 10(5):786-791.

Liu HR, Huang XQ, Lou DH, Liu XJ, Liu WK, Wang QA. 2014. Synthesis and acetylcholinesterase inhibitory activity of Mannich base derivatives flavokawain B. Bioorg Med Chem Lett. 24(19):4749-4753.

Lu J, Patel S, Sharma N, Soisson SM, Kishii R, Takei M, Fukuda Y, Lumb KJ, Singh SB. 2014. Structures of kibdelomycin bound to *Staphylococcus aureus* GyrB and ParE showed a novel U-shaped binding mode. ACS Chem Biol. 9(9):2023-31.

Nomura R, Nakano K, Nemoto H, Fujita K, Inagaki S, Takahashi T, Taniguchi K, Takeda M, Yoshioka H, Amano A, Ooshima T. 2006. Isolation and characterization of Streptococcus mutans in heart valve and dental plaque specimens from a patient with infective endocarditis. J Med Microbiol. 55(8):1135-1140.

Ohikhena FU, Wintola OA, Afolayan AJ. 2017. Evaluation of the Antibacterial and Antifungal Properties of *Phragmanthera capitata* (Sprengel) Balle (Loranthaceae), a Mistletoe Growing on Rubber Tree, Using the Dilution Techniques. Scientific World Journal. 2017:9658598.

Xiong G, Wu Z, Yi J, Fu L, Yang Z, Hsieh C, Yin M, Zeng X, Wu C, Lu A, et al. 2021. ADMETlab 2.0: an integrated online platform for accurate and comprehensive predictions of ADMET properties. Nucleic Acids Res. 49(W1):W5-W14.